IMS（Injection Molded Solder：溶融はんだインジェクション法）向け高耐熱性マスクレジストの開発

Development of liquid photoresist for IMS (Injection Molded Solder) with high thermal stability

武川　純[*1]　高橋　誠一郎[*2]　小畑　知弘[*3]　大喜多　健三[*4]　楠本　士朗[*5]
Jun Mukawa　　Seiichirou Takahashi　　Chihiro Kobata　　Kenzo Ohkita　　Shiro Kusumoto

長谷川　公一[*6]　青木　豊広[*7]　中村　英司[*7]　久田　隆史[*7]　森　裕幸[*7]　折井　靖光[*8]
Koichi Hasegawa　　Toyohiro Aoki　　Eiji Nakamura　　Takashi Hisada　　Hiroyuki Mori　　Yasumitsu Orii

　半導体実装業界において，高性能ICチップやパッケージの高密度実装を実現可能とする新たなバンピング技術が求められている．近年，IBMより，マスクレジストの開口部に溶融はんだを直接注入する，IMS（Injection Molded Solder：溶融はんだインジェクション法）と呼ばれる革新的なバンピングプロセスが提案された．本プロセスにおいて，マスクレジストには，約250 ℃の溶融はんだに対する耐熱性が求められる．著者らは，はんだが注入されていない開口部を残さず，100 ％のはんだ充填率を得るには，はんだ注入を阻害する，高温におけるマスクレジストからのアウトガス量の低減が重要であることを見出した．これらの知見をレジスト材料設計に反映させ，IMS向け新規高耐熱性マスクレジスト材料を開発した．

　Novel bumping technology that can realize high density assembly of IC chips and packages with a high number of I/O is required in the field of electronic packaging. Recently, a novel bumping technology called IMS (Injection Molded Solder) was proposed by IBM Corporation, which enabled direct injection of molten solder into the holes of a photoresist patterned array. In this process, photoresists which have thermal stability of up to 250 °C are required for surviving under direct contact with molten solders. To achieve 100 % solder filling into the photoresist holes, we must decrease outgassing from photoresists as it can prevent smooth solder filling at such elevated temperatures. Novel photoresists for IMS with high thermal stability were developed by reflecting such findings into the photoresist material design.

1 Introduction

　With the demand increasing significantly in big data for the Internet of Things（IoT），advanced packaging technology of 2.5D or 3DIC TSV structures and fan-out wafer level packaging technology have been studied and developed[1~5]. The interconnection in advanced packaging has recently begun being stacked in the z direction, so packaging structures and their fabrication processes have become more and more complicated. Also, the number of I/O and other functionalities of devices are increasing, which encourages downsizing of the metal wiring width/space and bump size/pitch.

＊1　2009年入社　先端電子材料開発室
＊2　2007年入社　筑波研究所
＊3　2008年入社　先端電子材料開発室
＊4　1994年入社　先端電子材料開発室
＊5　1992年入社　製造技術第二センター
＊6　1999年入社　先端電子材料開発室
＊7　　　　　　　日本アイ・ビー・エム株式会社
＊8　　　　　　　日本アイ・ビー・エム株式会社（論文執筆時の所属）

To date, solder bumps with sub-hundred micron sizes are generally fabricated by the electroplating method or the solder ball placement method. However, there are some limitations with these current bumping methods. For example, in the case of an electroplating method, the solder bump composition fabricated in this method is limited. Therefore, novel bumping processes are needed to satisfy the variety of recent requirements for high I/O density, fine bump pitch, novel solder bump composition, and further process cost reductions. Recently, a promising bumping process called "IMS (Injection Molded Solder)" was proposed [6]~[11]. In this process, molten solder is directly injected into holes patterned in photoresist mask films rather than carrying out conventional electroplating. One of the important advantages of the IMS process is its high and stable quality of solder bumps, because those obtained by electroplating can sometimes shift their composition unless there is careful maintenance of the electroplating solution conditions.

Our goal is to achieve perfect solder filling in a sub-hundred micron hole pattern array on 12-inch wafers with a simple IMS process. In order to achieve this, development of both photoresist materials and equipment for solder injection are essential. We are now collaborating with an equipment company, Senju Metal Industry Co., LTD., on the development of IMS technology.

In this study, the development status of liquid type photoresist for IMS process is described. Specifically, key material development points for achieving a 100 % solder filling rate by IMS technology are discussed. A Sn-3.0Ag-0.5Cu (SAC305) lead free solder with a melting point of 217 ℃ (solidus temperature), which is widely used in many applications in the industry, was chosen for this study. The thermal stability required in this process is much higher than that required for an electroplating method because the molten solder directly contacts the photoresist. In the beginning of this paper, the results of IMS defect analysis are described in detail. Then, the current development status for obtaining excellent solder filling is introduced. Finally, recent IMS trial status for obtaining finer patterns down to 40 μm pitch with 20 μm diameter holes is described.

2 Experiments

2.1 Design of the photoresist masks for IMS

JSR has been developing numerous kinds of photoresists for years. For the thickness range around ten to hundred microns, negative tone photoresist is an excellent choice for obtaining good lithographic patterns with good coating uniformity, a wide process margin during photolithography, enough strippability and high chemical stability [12], [13]. Based on these promising properties, negative tone photoresists were chosen as our first photoresist for IMS mask materials. A typical material design of negative tone photoresist for IMS and its cross linking image are shown in Figure 1.

It consists of a base polymer, cross linker, and photo initiator. The base polymer, which is the main component of photoresists, is an acrylic resin. It contains carboxylic groups as soluble units for alkaline developer and some other typical functional groups for adjusting mechanical, thermal, and optical properties of the polymer. The cross linker contains acrylic groups which enable it to make new bonds by UV irradiation. A radical type photo initiator, which is activated by ghi or i-line (365 nm) exposure, was selected.

As the photoresist is exposed to UV light, the photo initiator is activated and generates a radical species, which acts as a trigger for radical polymerization of vinyl groups in the cross linker. After UV exposure, a highly cross-linked structure is obtained, as shown in the right side of Figure 1, and becomes insoluble in alkaline developer. As a result, only the UV exposed areas remain on a substrate after the photoresist development. Such negative tone photoresists have been widely used as mask materials for electroplating of Cu, Ni, Au, or Sn/Ag for a long time. However, applying it to an IMS process is challenging from a thermal stability standpoint. In the case of using SAC305, the temperature during the process has to be higher than the melting point of SAC305.

In order to increase the thermal stability, some of the thermally unstable units in the original photoresist were removed and new units with high thermal stability were incorporated into the photoresist. In this paper, two kinds of photoresist, PR-1 as a standard type and PR-2 as a thermally-stable type, are described.
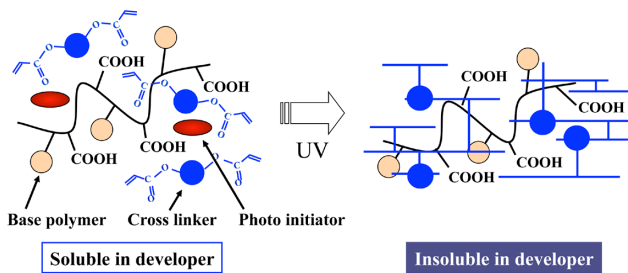
Figure 1 Cross linking image of the negative tone photoresists during UV exposure.

Figure 2 IMS (Injection Molded Solder) process.

2.2 Thermal stability analysis

During the IMS process, photoresists on wafers are exposed at temperatures at which the solder is completely molten. The amount of outgases from the photoresists at high temperature were evaluated by head-space gas chromatograph mass spectrometry (HS-GCMS). Photoresist-coated silicon wafers with exposure to UV light, and pre-heat treated at 200 ℃ for 10 or 20 minutes, were used as samples for HS-GCMS analysis. The samples were heated from 50 ℃ with a ramp rate of 10 ℃/min up to 250 ℃, then remained at 250 ℃ for 10 minutes. The cumulative amount of outgases from the photoresists were compared with different photoresist types and different pre-bake times.

2.3 IMS process flow

A schematic drawing of the IMS process flow is shown in Figure 2. The process is roughly divided into the following three steps.

The first step is the photoresist patterning process as shown in Figure 2 (1) - (3). Wafers used in this study were 4-, 6-, or 8-inch silicon with a thin copper layer deposited for conduction following the electroplating process as shown in Figure 2 (4). Photoresists were spin-coated onto copper deposited silicon wafers and baked at 120 ℃ for 5 minutes on a hot plate to remove organic solvents. Photoresist thickness was adjusted to around 50 μm by controlling the rotation speed of the spin coating. Then the coated photoresists were exposed under UV light (ghi-line or i-line) by photolithography at step (3) and immersed in a 2.38 % TMAH aqueous solution at room temperature for development. The wafers were rinsed with deionized water to remove the resid-
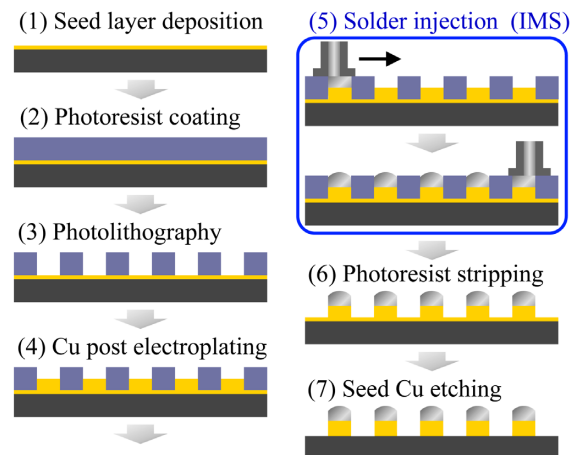
ual alkaline developer from the coatings, followed by heat treatment in an electric oven. Finally, photoresist masks with dense hole patterns (=1/1 hole/space pattern) and pitch from 40 to 150 μm were obtained.

The second step is the metal bumping fabrication process as shown in Figure 2 (4) - (5). Our target metal bumping structure is solder on 30 μm height copper posts, so the copper electroplating was conducted prior to the solder formation at IMS step. After fabricating the copper posts, IMS was conducted. The IMS head providing molten solder, SAC305, was placed on one side of the patterned wafer, as shown in Figure 2 (5). The head was then scanned to the other side of the wafer to complete the solder injection into holes of the photoresist masks.

The last step is the removal of photoresist and seed Cu process as shown in Figure 2 (6) - (7). The wafers with solder bumps were immersed into a conventional photoresist stripper, including TMAH and DMSO, at 50 ℃ for 20 minutes. Seed copper layer etching was carried out by immersing the wafer into a phosphoric acid-type etching solution.

2.4 Solder bump observation after IMS

The structure of the resulting metal bumping was observed using several types of microscopes. For the top view observation before and after stripping the photoresists, a conventional optical microscope was used. To check for the presence of any defects, where the injected solder didn't contact a pad and there is a gap between the solder and the pad, a contact-depth

mode scanning acoustic microscope (CSAM) was selected. Cross section observation was conducted by scanning electron microscope (SEM).

3 Results and Discussion

3.1 IMS defect analysis

As described in the previous paper [11], solder bumps with a diameter between 20 μm and 75 μm were successfully obtained by IMS technology using standard type PR-1 pre-baked at 200 ℃ for 10 minutes as a photoresist mask. However, the solder filling rate must be 100 % to be widely applied in industrial use. Figure 3 shows an example of bumping images with a solder filling defect after IMS. The defect in this figure was intentionally made under unoptimized IMS conditions. As shown in Figure 3 (a), both the holes, #1 and #2, look black from a top view observation, which mean that the solder was filled in the holes. However, the filling situation underneath the solders cannot be confirmed by such a top view. It can be confirmed by an observation from the bottom side using a CSAM. Two holes, #1 and #2, shown in Figure 3 (b), are totally different, whereas those two in Figure 3 (a) look similar.

In order to clarify the difference of the solder filling status, a sectional view observation was conducted. As shown in Figure 3 (c), the solder indicated by #2 reaches the bottom of the hole. However, it also indicates that #1 is confirmed to have non-contact to the pad underneath the solder.

3.2 Preparation of photoresist mask

From a series of solder bumping observations, we assumed that the generated outgases from the photoresists inside of the hole inhibited the solder filling. During the IMS process, wafers are exposed to temperature high enough that the solder is completely molten. In the case of SAC305, it reaches around 230 ℃, which is considered the melting point of SAC305. This information was our motivation to develop a novel thermally-stable photoresist with a lower amount of outgases, PR-2. Figure 4 shows the compositions of PR-1 and PR-2. The thermally unstable units in PR-1, functional unit "B" and photo initiator "D", were substituted to "C" and "E", respectively.

Figure 5 shows a comparison of the amount of outgases among different photoresists and pre-bake times at 200 ℃ measured by HS-GCMS analysis. The amount of outgas from Sample B (PR-2) is much less than that

Photo-resist	Base polymer			Photo initiator	
	A	B	C	D	E
PR-1 (Original)	✓	✓		✓	
PR-2 (Improved)	✓		✓		✓

Figure 4　The composition of PR-1 and PR-2.

Figure 5　Amount of outgas from photoresists pre-baked at 200 ℃ measured by HS-GCMS analysis.
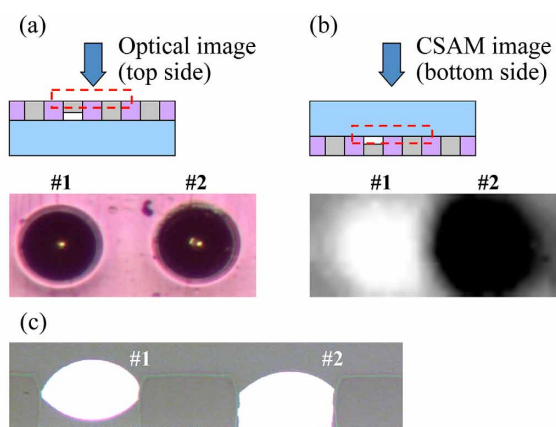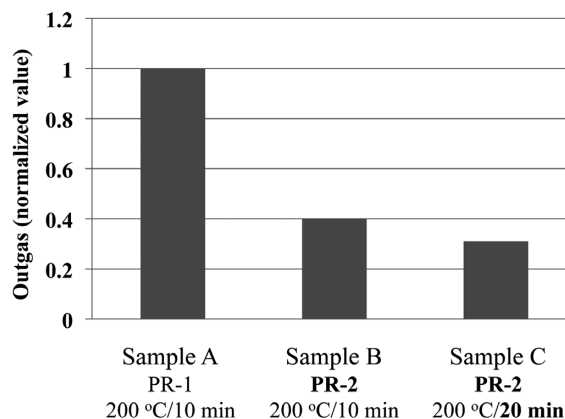

Figure 3　Example images of solder bumps processed with unoptimized IMS condition. (a) Top view by optical microscope, (b) Bottom view by CSAM, and (c) Sectional view by SEM.

from Sample A (PR-1). As shown in Sample C (PR-2), a longer pre-bake time that reduces residual volatiles also contributed to the decrease in the amount of outgases during the IMS process.

3.3 IMS demonstration

Figure 6 shows top view optical micrographs of solder bumps processed with the IMS method followed by photoresist stripping. Comparing the full shot images in Figure 6, the surface appearance of Sample B processed with PR-2 looks more uniform than that of Sample A processed with PR-1. In the same way, the surface appearance of Sample C pre-baked for 20 minutes looks more uniform than that of Sample B pre-baked for 10 minutes. These differences in appearance are caused by occurrences of missing solder. Magnified images corresponding to the white square in the full shot micrographs are shown on the right side of Figure 6. White arrows in these images indicate the holes without solder. In these holes, copper posts are directly observed. As we assumed, Sample C which generated

less outgases produced a higher solder injection ratio. In addition, other properties of the photoresists pre-baked at these conditions are summarized in Table 1.

There were no significant differences in the pattern profiles of the photoresists regardless of the photoresist types or the pre-bake temperatures. The elastic modulus and contact angle of each photoresist were also examined for a better understanding of the material properties during IMS. During the IMS process, an IMS head heated to around 230 ℃ is placed on the top surface of the patterned photoresists with the appropriate pressure, which may cause narrowing of the photoresist holes and make solder injection difficult. Therefore, the higher elastic modulus of PR-2 may also be one of the causes for achieving a better solder injection ratio. Further investigation is needed to clarify the effects of elastic modulus on solder filling rate.

We also measured the contact angle of water on the photoresists in order to understand the surface conditions. The measurement results show that each sample had a contact angle less than 30°, which means that the surface of each sample is hydrophilic and no significant difference was observed. However, we have not clarified the effect of the surface condition of the photoresist to solder injection solely from the results of a water contact angle measurement. Direct measurement of the contact angle with molten solder at IMS process temperature may be the best way to understand the effects of the photoresist surface condition. Further study is being conducted.

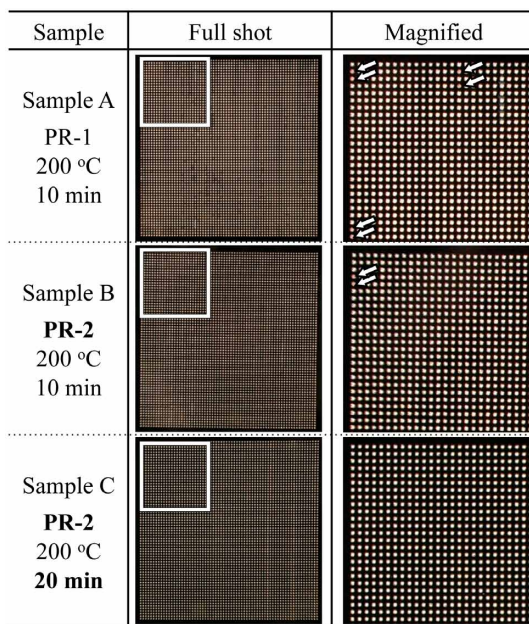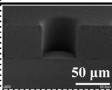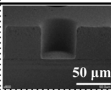| Sample	Full shot	Magnified
Sample A PR-1 200 ℃ 10 min		
Sample B **PR-2** 200 ℃ 10 min		
Sample C **PR-2** 200 ℃ **20 min**		

Figure 6 Top view optical micrographs of solder bumps processed with the IMS method followed by photoresist stripping. Left micrographs show the whole area of a single lithographic shot (hole/space=50 μm/50 μm). Right micrographs show the magnified images corresponding to the area highlighted with a white square in the left micrographs. White arrows show the defect points where no solder bumps were generated.

Table 1 Properties of photoresists pre-baked at 200 ℃

Sample	Sample A	Sample B	Sample C
Photoresist	PR-1	**PR-2**	**PR-2**
200 ℃ pre-bake	10 min	10 min	**20 min**
Pattern profile (FT=50 μm)	50 µm	50 µm	50 µm
Outgas level (normalized)	1.00	0.40	0.31
Elastic Modulus @250 ℃ [MPa]	27	52	52
Contact angle of water [°]	29	24	24

Through a series of experiments and discussion, as described above, we determined that PR-2 pre-baked at 200 ℃ for 20 minutes was the current best sample. Based on the findings so far, an IMS trial with 6-inch whole wafers and a solder filling rate evaluation were carried out. The results are shown in Figure 7. Each square column in Figure 7 expresses a 10×10 mm single lithographic shot, which has dense hole/space patterns (hole/space=1/1). There are three different hole diameters, 75 μm, 50 μm, and 40 μm, indicated upon the corresponding columns in the shot map. The number in each square column indicates the number of defects, where no solder was injected.

In the case of Sample B, PR-2 pre-baked at 200 ℃ for 10 minutes, no defects were observed at the shots with 75 μm hole size. However, some defects were observed at 50 μm hole size. Many more defects were observed for 40 μm diameter holes. In contrast, all the holes down to 50 μm in diameter were perfectly filled with solder in the case of Sample C, and only a few defects were generated in 40 μm holes. The solder filling rate was significantly improved with PR-2, which has higher thermal stability and less outgases than PR-1.

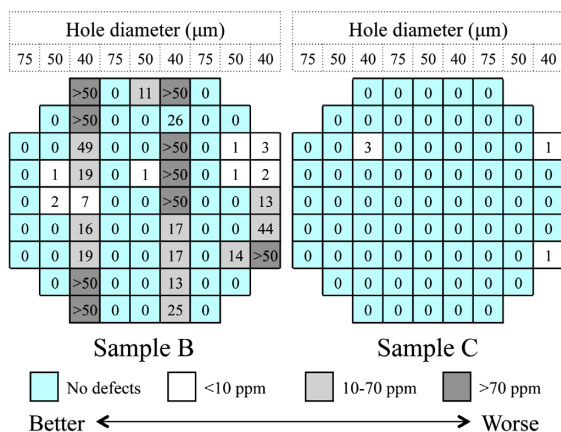Figure 8 shows a bird's eye view optical image that corresponds to the drawing in Figure 2 (7) of a solder bumped wafer by IMS with PR-2 after photoresist has been stripped and the seed copper layer etched. Solder has successfully been added to the tops of all the bumps. The solder on top of the copper post has excellent hemispherical shape immediately after the IMS head single scanning, without conducting a solder reflow process. This is one of the advantages for an IMS process versus conventional solder electroplating or solder ball placement methods.

Figure 9 shows a sectional view SEM micrograph of the corresponding bumped wafer. All the solder on top of the copper posts have almost the same height and shape. This height stability among bumps is likely derived from the excellent thickness uniformity of the
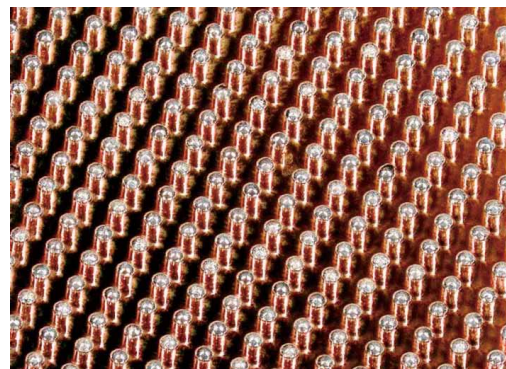

Figure 8 Bird's eye view image of solder bumps on copper post processed by IMS method. Photoresist, PR-2 pre-baked at 200 ℃ for 20 minutes, was used as the IMS mask material. Thickness of PR-2 used is 50 μm. Pattern pitch and hole diameter are 100 μm and 50 μm, respectively.
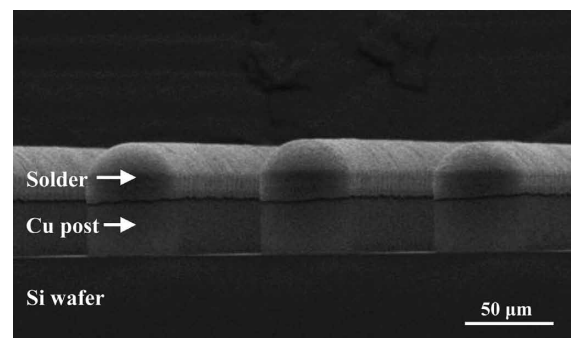

Figure 9 Side view image of solder bumps on copper posts processed by IMS method. Photoresist and process conditions used are identical with those used in Figure 8.

Hole diameter (μm)										Hole diameter (μm)								
75	50	40	75	50	40	75	50	40		75	50	40	75	50	40	75	50	40
		>50	0	11	>50	0						0	0	0	0	0		
	0	>50	0	0	26	0	0				0	0	0	0	0	0	0	
0	0	49	0	0	>50	0	1	3		0	0	3	0	0	0	0	0	1
0	1	19	0	1	>50	0	1	2		0	0	0	0	0	0	0	0	0
0	2	7	0	0	>50	0	0	13		0	0	0	0	0	0	0	0	0
0	0	16	0	0	17	0	0	44		0	0	0	0	0	0	0	0	0
0	0	19	0	0	17	0	14	>50		0	0	0	0	0	0	0	0	1
	0	>50	0	0	13	0					0	0	0	0	0	0		
		>50	0	0	25	0						0	0	0	0	0		

Sample B   Sample C

No defects   <10 ppm   10-70 ppm   >70 ppm

Better ←——————————————————→ Worse

Figure 7 Defect number map on a 6 inch whole wafer after IMS and photoresist stripping. Pre-bake time at 200 ℃ for Sample B was 10 minutes (left), and that for Sample C was 20 minutes (right). The numbers in each column indicate the number of defects in a single lithographic shot in 10x10 mm square. Each shot area is classified into four different categories and colors according to the frequency of defects.

photoresist used for IMS. In the case of conventional electroplating, there is often variation of solder height, which is caused by the size and shape variation of the photoresist holes or electric field strength variation within the wafer. The degree of solder height variation processed by electroplating is usually around ±5 %. Even though there is a certain degree of height variation in the copper posts underneath the solders, the variation after solder injection by IMS should decrease thanks to the high coating uniformity of the photoresist.

The promising solder bumping method, IMS for structures with 50 μm in diameter with very high solder filling rate, were described above. Hereafter, trials for obtaining finer pitch bumps are described. Optical micrographs of photoresists with finer pitch and corresponding bumps are shown in Figure 10. Finer pitch patterns, down to 20 μm in diameter with 50 μm thickness, were successfully obtained. Bumps corresponding to the shape of the photoresists were also obtained. Photoresist stripping and wet etching of the copper seed layer were also successfully carried out. However, as shown with Sample C in Figure 7, there are still some defects for bumps

with a diameter equal to or less than 40 μm. We will continue working to achieve perfect solder filling for finer pitch structures.

4 Conclusion

The current photoresist development status for, and its advantages for solder filling, were described. All the bumps down to 50 μm in diameter were perfectly filled with SAC305 as solder. Removing the thermally unstable unit in the base polymer contributed to a decrease of outgases in the IMS process and it enabled a stable solder filling. Excellent hemispherical shapes of the solders were obtained by a one time, simple IMS head scanning and without conducting a reflow process. Work for solder filling down to 20 μm is already underway with some success. Improvement in both photoresist materials and the IMS processes will continue to make the IMS technology more useful for practical high volume manufacturing.

Diameter	Photoresist	Solder bump
φ50 μm		
φ40 μm		
φ30 μm		
φ20 μm		

Figure 10 Photoresist pattern (left) and corresponding solder (Sn-3.0Ag-0.5Cu) bumps profile on copper post (right).

References

1) G. J. Jung, B. Y. Jeon, I. S. Kang: *Proc. EPTC 2009*, 191 (2009).

2) Y. Kurita, S. Matsui, N. Takahashi, K. Soejima, M. Komuro, M. Itou, C. Kakegara, M. Kawano, Y. Egawa, Y. Saeki, H. Kikuchi, O. Kato, A. Yanagisawa, T. Mitsuhashi, M. Ishino, K. Shibata, S. Uchiyama, J. Yamada, H. Ikeda: *Proc. ECTC 2007*, 821 (2007).

3) S. W. Yoon, Y. Lin, S. Gaurav, Y. Jin, V. P. Ganesh, T. Meyer, P. C. Marimuthu, X. Baraton, A. Bahr: *Proc. ECTC 2011*, 441 (2011).
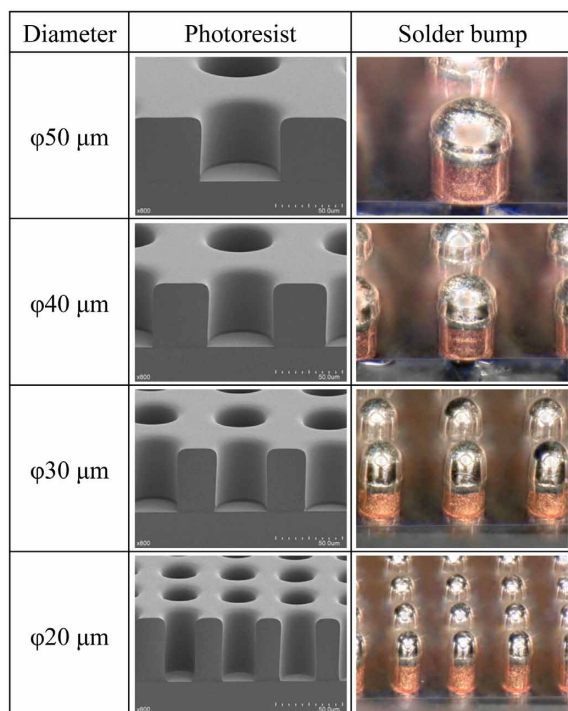
4) M. Santarini: *Xcell Journal*, **74**, 8 (2011).

5) M. Murugesan, H. Kino, H. Nohira, J. C. Bea, A. Horibe, F. Yamada, C. Miyazaki, H. Kobayashi, T. Fukushima, T. Tanaka, M. Koyanagi: *Proc. IEDM 2010*, 231 (2010).

6) P. A. Gruber, D. Y. Shih, L. Belanger, G. Brouillette, D. Danovitch, V. Oberson, M. Turgeon, H. Kimura: *Proc. ECTC 2004*, 650 (2004).

7) E. D. Perfecto, D. Hawken, H. P. Longworth, H. Cox, K. Srivastava, V. Oberson, J. Shah, J. Garant: *Proc. ECTC 2008*, 1641 (2008).

8) J. W. Nah, P. A. Gruber, P. A. Lauro, D. Y. Shih, K. Toriyama, Y. Orii, H. Noma, T. Nishio: *Proc. ECTC 2009*, 61 (2009).

9) J. W. Nah, P. A. Gruber, P. A. Lauro, C. Feger: *Proc. IMAPS 2010*, 348 (2010).

10) J. W. Nah, J. Gelorme, P. Sorce, P. Lauro, E. Perfecto, M. Mcleod, K. Toriyama, Y. Orii, P. Brofman, T. Nauchi, A. Takaguchi, K. Ishiguro, T. Yoshikawa, D. Daily, R. Suzuki: *Proc. ECTC 2014*, 1308 (2014).

11) T. Aoki, K. Toriyama, H. Mori, Y. Orii, J. W. Nah, S. Takahashi, J. Mukawa, K. Hasegawa, S. Kusumoto, K. Inomata: *Proc. IMAPS 2014*, 713 (2014).

12) H. Akimaru, H. Ishikawa, H. Sakakibara, S. Naruse, K. Okamoto, K. Inomata: *Proc. ICEP 2014*, 131 (2014).

13) H. Sakakibara, H. Akimaru, A. Hiro, K. Sato, K. Fujiwara, K. Okamoto, S. Kusumoto: *Proc. ICEP 2015*, 628 (2015).